Nondestructive optical detection of monomer uptake in wood polymer composites

Andrea Farina,[1,*] Ilaria Bargigia,[2] Emma-Rose Janeček,[3] Zarah Walsh,[3] Cosimo D'Andrea,[1,2,4] Austin Nevin,[1] Michael Ramage,[5] Oren A. Scherman,[3] and Antonio Pifferi[1]

[1]*Consiglio Nazionale delle Ricerche, Istituto di Fotonica e Nanotecnologie, Piazza L. Da Vinci 32, I-20133 Milano, Italy*

[2]*Politecnico di Milano, Dipartimento di Fisica, Piazza L. Da Vinci 32, I-20133 Milano, Italy*

[3]*Melville Laboratory for Polymer Synthesis, Department of Chemistry, University of Cambridge, Lensfield Road, CB2 1EW, UK*

[4]*Center for Nano-Science and Technology @Polimi, Istituto Italiano di Tecnologia, via G. Pascoli 70/3, 20133 Milano, Italy*

[5]*Department of Architecture, University of Cambridge, UK*

**Corresponding author: andrea.farina@polimi.it*

Received October 10, 2013; revised November 27, 2013; accepted November 29, 2013;
posted December 3, 2013; published January 6, 2014

The assessment and monitoring of the impregnation of wood by functional monomers is important in various fields, particularly in the timber industry and conservation, where nondestructive monitoring is particularly appealing. In the timber industry, for example, wood may be treated with preservatives, which can improve the wood's biological resistance and dimensional stability [1–3], allowing its use in the construction of buildings and for a wealth of interior design applications (flooring, furniture and fixtures, for example). While in the conservation of archaeological wooden artifacts, it is common to apply polymeric consolidants to aged and degraded wood in order to strengthen structures (for example excavated wooden ships, or sarcophagi) [4,5], or to stabilize damaged worm-eaten wood, which is common in the restoration of wooden furniture and wooden panel paintings [6]. Despite the prevalence of consolidated wood, there are few techniques that allow the assessment of the penetration of polymeric materials in the complex structure of wood, which compromises the optimization of impregnation, and the determination of the heterogeneity of treated objects, which may require restoration in the future.

Various techniques are currently used for the study and characterization of the internal structure of wood and are based on x ray, solid and solution state nuclear magnetic resonance, ultrasound, and microwave [7]. Techniques that exploit optical radiation in the near infrared spectrum have also been employed for the characterization of wood. In particular, standard near infrared spectroscopy, widely used for the chemical and physical characterization of wood, is based on the accurate detection of an attenuation spectrum obtained in reflectance over a wide spectral range in the near- or mid-infrared region with continuous wave light sources [8,9]. Because of the high scattering of light in wood [10], these spectra do not provide a quantification of the concentration of the absorbing species and a huge effort in statistical and multivariate analysis must be employed to correlate spectral variations to chemical or structural changes. Another technique based on optical radiation [GAs in Scattering Media Absorption Spectroscopy (GASMAS)] has been used for the monitoring of water vapor in wood during the drying process [11,12]. This technique is based on the combination of tunable diode laser spectroscopy (TDLAS) with the physics of light propagation in diffusive media for the estimation of gas content inside the wood [13].

Recently, another noninvasive technique based on near-infrared radiation has been proposed for the characterization of wood and moisture content (MC) known as time-resolved diffuse optical spectroscopy (TRS) [10,14]. Initially proposed for the characterization of biological tissues, TRS allows the simultaneous determination of the absorption and scattering properties of a medium allowing the subsequent quantification of wood composition without any multivariate analysis. Near-infrared radiation has also the advantage of a longer penetration depth compared to mid-infrared, thus allowing a noninvasive characterization of wood centimeters below the surface. A picosecond monochromatic pulse is injected into the sample and collected from another location on its external surface. The temporal profile of the detected pulse carries information about absorption and scattering. In particular, the probability of absorption is related to the asymptotic slope of the detected pulse, while scattering affects the delay of the detected pulse.

By injecting a monochromatic pulse at different wavelengths over a broad spectral range, it is possible to recover information on key constituents in the wood from the absorption spectrum and on the structure of the material from the scattering spectrum. TRS is a noninvasive, rapid technique and can be adapted for *in situ* applications.

Herein we apply TRS for the nondestructive monitoring of monomer uptake inside a wooden matrix. In

particular, we used the absorption spectrum of a monomer mixture to estimate its local concentration inside the wood matrix. The TRS system, described in detail elsewhere [15,16], is depicted in Fig. 1. It consists of a pulsed supercontinuum source (SuperK Extreme, NKT) emitting mode-locked laser pulses in the range 450–1750 nm at a repetition rate of 40 MHz. The white light exiting the source is dispersed by an SF10 Pellin–Broca prism and then focused on a variable slit by a 150 mm focal length achromatic doublet for better spectral bandwidth selection. Tuning is achieved by the automated rotation of the prism. The slit plane is imaged on a 50 μm graded index fiber by two achromatic lenses. The spectral bandwidth of the system ranges from about 6 nm at 900 nm to 15 nm at 1300 nm. Light is delivered to and collected from the sample by means of 1 mm step index fibers. The detector is a photomultiplier tube (PMT) (Hamamatsu-H10330A-45) with a quantum efficiency of about 2% in the range 900–1300 nm. The instrumental response function (IRF), measured facing both detection and injection fibers, has a FWHM of about 300 ps over the whole spectral range. The time-of-flight (TOF) distribution of detected photons is measured by a time-correlated single photon counting board mounted on the PC, which controls both the prism rotation and the data acquisition. The whole system, comprising power source, detector, laser source, and PC, is mounted on a rack trolley, and it is portable and suitable for *in situ* measurements.

Samples consist of four spruce pieces cut into a parallelepipeds (1 cm × 1 cm × 10 cm) with wood fibers approximately running parallel to the longer dimension.

In order to probe the monomer uptake right in the middle of the sample, we measured the samples in collinear transmittance geometry with injection- and collection-fiber axis perpendicular to the longer side placed at 5 cm from the edge. The TOF distributions were acquired for 10 s at each wavelength, setting the laser power as to reach a count rate of about 400 kcounts/s. The rotation of the prism was adjusted to sample the spectral range between 900 and 1350 nm in steps of 10 nm.

For each wavelength we analyzed the photon TOF distribution by fitting the data to the time-resolved analytical expression derived for a solution of the radiative transfer equation under the diffusion approximation for a laterally infinite slab with extrapolated boundary conditions [17]. The refractive index of treated and untreated spruce has been set to 1.17 based on its porosity (~70%), on the refractive index of its solid part (~1.53) and on the MC of about 10% at room temperature with a relative humidity

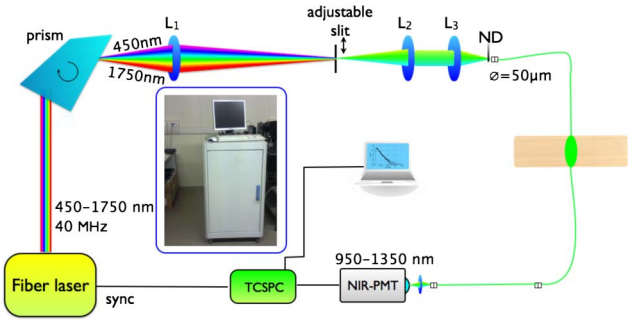

Fig. 1. Schematic of the setup.

of 55% [18]. The fitting range included photons producing a count rate higher then 80% of the peak on the trailing edge and 1% on the leading edge. The range does not include early photons to better fulfill the diffusion approximation. The fitting method was based on a Levenberg–Marquardt algorithm [19]. At each iteration of the fitting procedure, the IRF is convoluted with the theoretical model.

First we measured the absorption spectrum of the wood samples in the range 900–1350 nm before impregnation. Then we prepared a monomer mixture (named MIX hereafter) of glycidyl methacrylate (GMA) (45%), methylmethacrylate (MMA) (45%), and ethylene glycol dimethacrylate (EDMA) (10%) and we measured its extinction coefficient using a standard spectrophotometer (JASCO V-570) in the range 400–2000 nm. Each piece of wood was then immersed in MIX and a vacuum (~1 mbar) was applied for more than 30 min. The vacuum was then released and the wood allowed to sit in the MIX for more than 1 h. The samples were removed from the bath and measured again in the same marked positions as the first measurements.

The capability of TRS to detect the monomer uptake into the wood matrix is demonstrated in Fig. 2. The absorption spectra of sample A before (circle) and after (triangle) MIX impregnation are shown together with their difference (squares) and the MIX spectrum taken at the spectrometer (line, right axis). The spectral shape of the absorption difference, with a broad maximum around 1130–1180, closely matches the pure mix spectrum, thus proving the sensitivity of TRS to the wood impregnation.

The two main absorption bands around 1000 and 1200 nm in the untreated wood is due to the combination of water and cellulose. The absorption with the greatest relative change following impregnation, and that hence provides best contrast for monitoring the MIX uptake in wood, is around its absorption maximum at 1190 nm.

The quantitative assessment of MIX uptake can be achieved using the Beer Lambert law [20]:

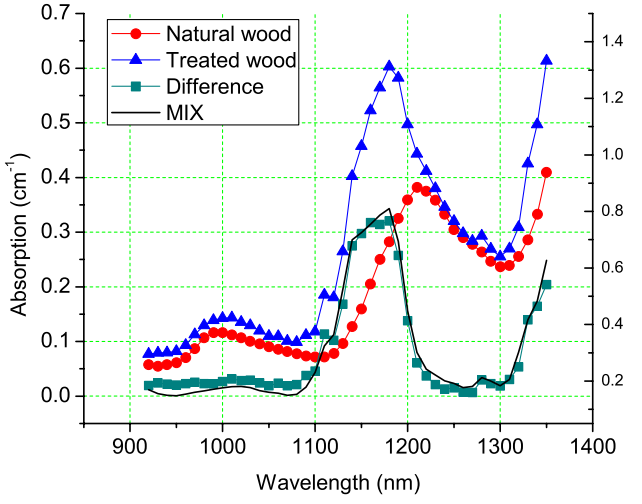

Fig. 2. Absorption spectra of sample A before (natural wood) and after the treatment. MIX absorption is also shown together with the difference in A before and after treatment.

$$\mu_a(\lambda) = \sum c_i \epsilon_i(\lambda), \quad (1)$$

where $\mu_a(\lambda)$ is the absorption spectrum, c_i are the component concentration, and $\varepsilon(\lambda)$ represents the reference spectrum of the ith component. As components, we considered the spectra from untreated wood (taken as a combination of water, lignin, cellulose, and extractives), the MIX, and water. Yet, for an accurate quantification, MIX-related changes in refractive index must be properly addressed. Indeed, the replacement of air by the monomer decreases the light speed in the medium and thus affects the photon TOF distribution dependently on the (unknown) monomer concentration.

To overcome this problem, we started by observing that, due to the exponential factor $\exp[-(\mu_a/n)ct]$, where μ_a is the absorption coefficient, n the refractive index of the diffusive media, c is the light speed in vacuum, and t is the time [17], the ratio μ_a/n is approximately constant. Consequently it is possible to estimate the absorption at a different refractive index without performing a new TR fit. We inserted the refractive index estimation directly into the spectra analyses using recursive equations for refractive index and absorption spectrum. In detail:

$$n^{(1)} = n^{(0)} + \sum_i \Delta\rho_i n_i \quad (2)$$

$$\mu_a^{(1)} = \mu_a^{(0)} + \sum_i \Delta\rho_i \epsilon_i, \quad (3)$$

where "0" and "1" refer to samples taken before and after the treatment, respectively, $\Delta\rho_i$ is the concentration change after the treatment, n_i the refractive index, and ϵ_i is the extinction coefficient of the ith component. In our case the components are: the solid part of wood composed of lignin and cellulose (w), water (H_2O), air, and mix. We assume the absorption spectrum of wood before the treatment to be

$$\mu_a^{(0)} = \rho_w^{(0)} \epsilon_w + \rho_{H_2O}^{(0)} \epsilon_{H_2O}. \quad (4)$$

We observe that the quantities $\rho_{H_2O}^{(0)}$ and $\rho_w^{(0)}$ are related to the initial MC and to the porosity, respectively. Equations (2), (3), and (4) can be used to estimate $\Delta\rho_w$, $\Delta\rho_{H_2O}$, and $\rho_{mix}^{(1)}$ with the constraint that

$$\sum_i \Delta\rho_i = 0. \quad (5)$$

The absorption spectrum of treated wood is rescaled considering $n^{(1)}$ at every iteration. The fitting procedure minimizes the difference between $\mu_a^{(1)}$ and the measured spectrum of treated wood by changing $\Delta\rho_w$, $\Delta\rho_{H_2O}$, and $\rho_{mix}^{(1)}$. The reduced scattering coefficient μ_s' can be estimated by observing that the product $\mu_s' n$ remains approximately constant. As the reduced scattering also affects the boundary conditions, the approximation is valid only for small changes of refractive index. Thus we decided to use the estimated refractive indices to reestimate the correct scattering coefficients with a TR fit. Results of this second-level fitting procedure are reported in Table 1. For completeness the mass increase for unit volume is also shown.

It is worth noting a negligible change in water and wood content in all samples, meaning that the MC and the volume are almost constant. While it is not possible to compare MIX content directly with mass increase, because of the uneven uptake and distribution of polymer, values of MIX content suggest that the major differences observed in samples reflect differences in the mass increase (and hence overall monomer uptake). These differences are in good agreement with the expected natural variations in wood samples. However, it is noted that analysis of points in the center of the piece of wood suggests a lower concentration of monomer than that measured through change in mass. Refractive indexes increase accordingly to the MIX content.

The scattering spectrum is almost constant, indicating that the average fiber size is larger than the probing wavelength, as discussed elsewhere [10]. Scattering values are shown in Table 1 for samples before and after the treatment. We observe a scattering reduction for all samples. Scattering in wood is physically caused by a local refractive index mismatch between air and the wood matrix. After impregnation the monomer fills the empty intra-fiber space, thus reducing the refractive index mismatch and yielding a lower scattering coefficient. In addition to absorption, scattering is strongly sensitive to the monomer presence, as can be seen for sample B where there is a greater reduction in the scattering, indicating a greater uptake of monomer.

Because of the high diffusivity of light through wood, values discussed above should be considered as an average over the volume probed by light inside the sample. We performed a Monte Carlo simulation of light propagation in a homogeneous slab (1 cm thickness) in collinear transmittance geometry having the same measured optical properties [21]. Results show that the received photons trajectories probe a volume having a lateral extension of about 5 mm and also that our measurements are not affected by boundary effects along the short dimensions.

In conclusion, we have shown that by using TRS it is possible to monitor the uptake of a monomer inside a

Table 1. Estimated Quantities from Samples after Treatment in MIX[a]

Sample	Δ [Mass] (g/cm^3)	[MIX] (g/cm^3)	Δ [H_2O] (g/cm^3)	Δ [Wood] (%)	Δ [Air] (%)	$n^{(1)}$	$\mu_s'^{(0)}$ (cm^{-1})	$\mu_s'^{(1)}$ (cm^{-1})
A	0.488	0.483	0.003	−3.5	−44.8	1.60	154	33
B	0.445	0.337	0.008	−3.1	−31.2	1.52	168	82
C	0.326	0.166	−0.003	−1.5	−14.6	1.34	180	109
D	0.159	0.022	−0.001	−0.3	−1.8	1.20	146	115

[a]Δ [MIX], Δ [H_2O], Δ [Wood], Δ [Air], $n^{(1)}$ are estimated using the method described by Eqs. (2)–(5), Δ [Mass] by weighing the samples before and after the treatment, $\mu_s'^{(0)}$ and $\mu_s'^{(1)}$ using the TR fitting. In particular $\mu_s'^{(1)}$ is estimated using $n^{(1)}$ as refractive index.

wood matrix. The technique relies on *a priori* information about the monomer absorption spectrum and can be extended in a more general way to the monitoring of the uptake of any external material inside any porous matrix. Future research will seek to exploit TRS for assessment of differences in uptake in time, and the analysis of historical samples.

The authors would like to thank Patrick Fleming for stimulating discussions and comments on earlier drafts of the manuscript. The research leading to these results has received funding from LASERLAB-EUROPE (grant agreement no. 284464, EC's Seventh Framework Programme), EPSRC, ERC Starting investigators grant (AS-PiRe, 240629), and the Walters Kundert Charitable Trust.

References

1. M. K. Dubey, S. Pang, and J. Walker, Holzforschung **66**, 49 (2012).
2. S. Donath, H. Militz, and C. Mai, Wood Sci. Technol. **38**, 555 (2004).
3. C. A. S. Hill, S. C. Forster, M. R. M. Farahani, M. D. C. Hale, G. A. Ormondroyd, and G. R. Williams, Int. Biodeterior. Biodegradation **55**, 69 (2005).
4. J. Glastrup, Y. Shashoua, H. Egsgaard, and M. N. Mortensen, Macromol. Symp. **238**, 22 (2006).
5. M. N. Mortensen, H. Egsgaard, S. r. Hvilsted, Y. Shashoua, and J. Glastrup, J. Archaeol. Sci. **34**, 1211 (2007).
6. B. New and R. Marchant, in *Facing Challenges of Panel Paintings Conservation Trends, Treatment, and Training*, A. Phenix and S. A. Chui, eds. (Getty Conservation Institute, 2011), pp. 36–47.
7. V. Bucur, Meas. Sci. Technol. **14**, R91 (2003).
8. S. Tsuchikawa, Appl. Spectrosc. Rev. **42**, 43 (2007).
9. H. Kobori, N. Gorretta, G. Rabatel, V. Bellon-Maurel, G. Chaix, J.-M. Roger, and S. Tsuchikawa, Holzforschung **67**, 307 (2012).
10. C. D'Andrea, A. Farina, D. Comelli, A. Pifferi, P. Taroni, G. Valentini, R. Cubeddu, L. Zoia, M. Orlandi, and A. Kienle, Appl. Spectrosc. **62**, 569 (2008).
11. M. Andersson, L. Persson, M. Sjöholm, and S. Svanberg, Opt. Express **14**, 3641 (2006).
12. I. Bargigia, A. Nevin, A. Farina, A. Pifferi, C. D'Andrea, M. Karlsson, P. Lundin, G. Somesfalean, and S. Svanberg, J. Near Infrared Spectrosc. **21**, 259 (2013).
13. G. Galbács, Appl. Spectrosc. Rev. **41**, 259 (2006).
14. C. D'Andrea, A. Nevin, A. Farina, A. Bassi, and R. Cubeddu, Appl. Opt. **48**, B87 (2009).
15. A. Bassi, A. Farina, C. D'Andrea, A. Pifferi, G. Valentini, and R. Cubeddu, Opt. Express **15**, 14482 (2007).
16. I. Bargigia, A. Tosi, A. Bahgat Shehata, A. Della Frera, A. Farina, A. Bassi, P. Taroni, A. Dalla Mora, F. Zappa, R. Cubeddu, and A. Pifferi, Appl. Spectrosc. **66**, 944 (2012).
17. F. Martelli, S. Del Bianco, A. Ismaelli, and G. Zaccanti, *Light Propagation through Biological Tissue and Other Diffusive Media* (SPIE, 2010).
18. H. Juttula and A. J. Makynen, in *Instrument Measurement Technology Conference* (IEEE, 2012), pp. 1–4.
19. W. H. Press, S. A. Teukolsky, W. T. Vetterling, and B. P. Flannery, *Numerical Recipes: The Art of Scientific Computing* (Cambridge University, 1988).
20. A. Pifferi, A. Farina, A. Torricelli, G. Quarto, R. Cubeddu, and P. Taroni, J. Near Infrared Spectrosc. **20**, 223 (2012).
21. E. Alerstam, T. Svensson, and S. Andersson-Engels, J. Biomed. Opt. **13**, 1 (2008).